1

Repeatability of adaptation in sunflowers: genomic regions harbouring inversions also

drive adaptation in species lacking an inversion

4

Shagheyegh Soudi[1+], Mojtaba Jahani[1,2+], Marco Todesco[2,3,4], Gregory L. Owens[5], Natalia

Bercovich[2], Loren H. Rieseberg[2], Sam Yeaman[1,*]

7

+Joint first-authors

9

Author affiliations:

1. Department of Biological Sciences, University of Calgary, 2500 University Drive NW, Calgary, Canada, T2N 1N4
2. Department of Botany, University of British Columbia, 6270 University Blvd, Vancouver, Canada, V6T 1Z4
3. Michael Smith Laboratories, University of British Columbia, 6270 University Blvd, Vancouver, Canada, V6T 1Z4
4. Irving K. Barber Faculty of Science, University of British Columbia Okanagan, 3187 University Way, Kelowna, Canada, V1V 1V7
5. Department of Biology, University of Victoria, 3800 Finnerty Rd, Victoria, Canada, V8P 5C2

21

*corresponding author: Sam Yeaman, samuel.yeaman@ucalgary.ca

23

24

1

Abstract

Local adaptation commonly involves alleles of large effect, which experience fitness advantages when in positive linkage disequilibrium (LD). Because segregating inversions suppress recombination and facilitate the maintenance of LD between locally adapted loci, they are also commonly found to be associated with adaptive divergence. However, it is unclear what fraction of an adaptive response can be attributed to inversions and alleles of large effect, and whether the loci within an inversion could still drive adaptation in the absence of its recombination-suppressing effect. Here, we use genome-wide association studies to explore patterns of local adaptation in three species of sunflower: *Helianthus annuus*, *H. argophyllus*, and *H. petiolaris*, which each harbour a large number of species-specific inversions. We find evidence of significant genome-wide repeatability in signatures of association to phenotypes and environments, which are particularly enriched within regions of the genome harbouring an inversion in one species. This shows that while inversions may facilitate local adaptation, at least some of the loci involved can still make substantial contributions without the benefit of recombination suppression. While a large number of genomic regions show evidence of repeated adaptation, most of the strongest signatures of association still tend to be species-specific, indicating substantial genotypic redundancy for local adaptation in these species.

Introduction

The genetic basis of local adaptation is sometimes highly repeatable, with examples of large effect genes driving responses in multiple species, such as *FT* affecting flowering time in numerous plants (Izawa 2007; Auge et al. 2019) or *Mc1r* driving colour polymorphisms in vertebrates(Manceau et al. 2010; Rosenblum et al. 2014). Local adaptation can also be repeated for polygenic traits, with significant patterns of similar association found across many loci for comparisons of conifers (Yeaman et al. 2016), maize and its wild relative teosinte (Tittes et al. 2021; Wang et al. 2021), and *Brassicaceae* (Bohutínská et al. 2021), to name a few. While we have a growing number of examples of repeatability in the basis of adaptation, it is also interesting to know if species use different genes to adapt to the same selection pressure. Genotypic redundancy – the potential for many genotypes to yield a given phenotype -- is one critical factor affecting the repeatability of adaptation, as high redundancy would be expected to result in lower repeatability (Yeaman et al. 2018). Another critical factor affecting repeatability

2

56   is shared standing variation, whether present due to introgression or incomplete lineage sorting.

57   In either case, variants shared among lineages are much more likely to contribute to a repeated

58   response than new mutations (MacPherson and Nuismer 2018; Ralph and Coop 2015).

59   Consistent with this, Bohutínská and colleagues (2021) found that repeatability was negatively

60   related to phylogenetic distance. While we are now accumulating more studies about the

61   repeatability of adaptation, we still have very few examples and much remains unknown about

62   the relative importance of these factors (Yeaman 2022).

63

64   Inversions have been implicated in local adaptation in many species (Wellenreuther and

65   Bernatchez 2018), likely due to their effect to suppress recombination between any causal loci

66   within their bounds (Rieseberg 2001; Noor et al. 2001; Kirkpatrick and Barton 2006). Despite

67   mounting evidence of their importance in adaptation, it is unclear how inversions may covary

68   with repeatability of adaptation among species. If most alleles have small effects relative to

69   migration rate and can only contribute to local adaptation via the benefit of the recombination-

70   suppressing effect of an inversion, then we would expect little repeatability at the site of an

71   inversion – other species lacking the inversion would not tend to use that same region for

72   adaptation. On the other hand, if some loci are particularly important for local adaptation and

73   regularly yield mutations of large effect, with these patterns being conserved among species,

74   repeatability within regions harbouring inversions may be substantial.

75

76   Here, we explore the repeatability of local adaptation in three species of sunflowers, *Helianthus*

77   *annuus*, *Helianthus argophyllus* and *Helianthus petiolaris* (Figure 1), which harbour large

78   regions of suppressed recombination ("haploblocks"), most of which are likely inversions, and

79   are often associated with adaptive traits (Todesco et al. 2020). *Helianthus annuus*, the common

80   sunflower, is the closest wild relative of cultivated sunflower, which was domesticated from it

81   around 4,000 years ago (Blackman et al. 2011). Populations of *H. annuus* are distributed

82   throughout the central and western USA and generally found on mesic soils, but can grow in a

83   variety of disturbed or extreme habitats, such as semi-desertic or frequently flooded areas, as

84   well as salt marshes. *Helianthus petiolaris*, the prairie sunflower, prefers sandier soils, and

85   ecotypes of this species are adapted to sand sheets and sand dunes (Ostevik et al. 2016). Here we

86   include samples from two subspecies: *H. petiolaris ssp. petiolaris*, which is commonly found in

3

87   the southern Great Plains, and *H. petiolaris ssp. fallax*, which is limited to more arid regions in

88   Colorado, Utah, New Mexico and Arizona (Heiser et al. 1969). *Helianthus petiolaris* and *H.*

89   *annuus* have broad and overlapping distributions throughout the central and western United

90   States and appear to have adapted to similar changes in temperature, moisture and photoperiod

91   regimes. There is also evidence indicating *H. annuus* and *H. petiolaris* have likely been

92   exchanging genes during much of their history of divergence (Strasburg and Rieseberg 2008),

93   although partially isolated by strong pre- and post-zygotic barriers (Sambatti et al. 2012). The

94   third species, *Helianthus argophyllus*, the silverleaf sunflower, is found exclusively in the

95   southeast coast of Texas and includes both an early flowering ecotype on the coastal barrier

96   islands and a late flowering ecotype inland (Moyers and Rieseberg 2016; Todesco et al. 2020).

97   *H. argophyllus* is thought to have undergone cycles of sympatry and allopatry with *H.*

98   *annuus* and *H. petiolaris* over time, but currently only overlaps with *H. annuus,* which is likely

99   recent (Heiser, 1951).

100

101   Using broad sampling across the ranges of these species (Figure 1), we study the genomic

102   basis of local adaptation by conducting genome-wide scans for associations with climatic and

103   soil environmental variables and phenotypes measured in a common garden. An inherent

104   problem in studying the basis of local adaptation is accounting for the covariance between

105   genome-wide population genetic structure and environment. When the selection pressure driving

106   local adaptation tends to parallel a main axis of demographic expansion or isolation by distance,

107   neutral alleles will have spatial patterns resembling those of causal alleles. Methods that do not

108   correct for population structure have large numbers of false positives because allele frequencies

109   at neutral loci tend to correlate with the environment more than expected by chance (Lotterhos

110   and Whitlock 2014). By contrast, methods that use structure correction tend to suffer from false

111   negatives because the causal loci have similar patterns of allele frequency variation as the

112   genomic background, and so their statistical signatures are decreased (DeRaad et al. 2021).

113   When a non-corrected approach is applied to multiple species, the false positive problem can be

114   mitigated when testing for loci that contribute to repeated adaptation, as the same gene should

115   not tend to be a false positive in multiple species more often than expected by chance (Yeaman

116   et al. 2016). Here we use a conventional GWAS approach with structure correction to study the

117   basis of phenotypes, which vary both within and among populations, and use an uncorrected

118   approach to test association to environment, which only varies among populations. For the

119   environmental association portions of the study, we also explore the effect of structure correction

120   in some analyses, to contrast the false negative vs. false positive problem inherent in each

121   approach. We apply these approaches individually to *H. annuus*, *H. argophyllus*, and the two *H.*

122   *petiolaris* subspecies, and make pairwise and higher-order comparisons among combinations of

123   these four lineages to study repeatability.

124

125   Our overall aim is to characterize the extent of repeatability of local adaptation for different traits

126   and environments, and explore the importance of various factors that may drive differences in

127   repeatability. We begin by using the strength of phenotype-environment correlations to identify

128   which environmental variables are most important in driving local adaptation within each

129   species, and use an index to quantify the relative similarity in these patterns among pairs of

130   species. We then use methods similar to Yeaman et al. (2016) to identify regions of the genome

131   that exhibit greater similarity in signatures of association among pairs of lineages than expected

132   by chance, and explore how the number and total size of these regions covaries with the index of

133   similarity in environmental importance. We also explore whether these regions of repeated

134   adaptation tend to covary with patterns of shared standing variation and test if they are enriched

135   within previously identified haploblocks, to explore the role of inversions in adaptation. We then

136   identify candidate genes that show particularly strong signatures of repeated adaptation across

137   multiple lineages and test whether they tend to share common Gene Ontology terms indicating

138   similar function. Finally, based on the number of signatures of adaptation that are shared vs. non-

139   shared among lineages, we estimate the number of regions genome-wide that could potentially

140   contribute to local adaptation for each variable and phenotype, which is related to the genotypic

141   redundancy. Taken together, our results show that local adaptation in sunflowers tends to involve

142   both strong repeatability at a small number of genes, often associated with inversions, coupled

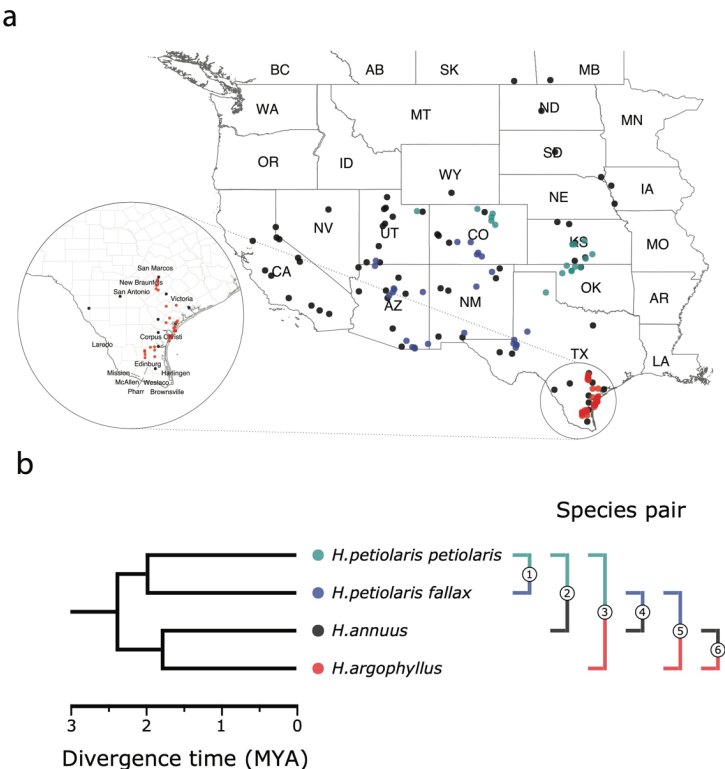143   with high redundancy and non-repeated responses across a much larger number of loci.

144

145

146

147

5

a

b

148
149 **Figure 1. Sampling sites and phylogenetic relationship among surveyed species.**
150 (a), sampling locations of wild sunflower populations studied in the present study. (b)
151 phylogenetic relationship of the four (sub-)species. Numbered brackets represent the six pairwise
152 comparisons performed in this study.
153

154

155

156 **Results**

157 **Local adaptation at the phenotypic level.** The four taxa vary considerably in the breadth of

158 environmental variation spanned by their respective ranges, with *H. annuus* spanning the widest

159 niche and *H. argophyllus* spanning the narrowest (Figure 2A). Local adaptation is quite

160 pronounced, as exhibited by strong correlations for many combinations of phenotypes and

161 environmental variables (Figure S1). To quantify the similarity in patterns of local adaptation

162 among pairs of species, for each environmental variable we calculate an index we refer to as the

163 Similarity in Phenotype-Environment Correlation (SIPEC), which is maximized when both

164 species have strong correlations with the environmental variable across many phenotypes (see

6

165   Methods). To prevent heavily weighting the contribution of multiple highly correlated

166   phenotypes, we fit a principal components analysis to the phenotypes and used the resulting axes

167   to calculate SIPEC. We find the largest values of SIPEC for temperature variables and the

168   smallest values for soil types, and generally find higher values for comparisons between the

169   *petiolaris* subspecies (Figure S2).

170
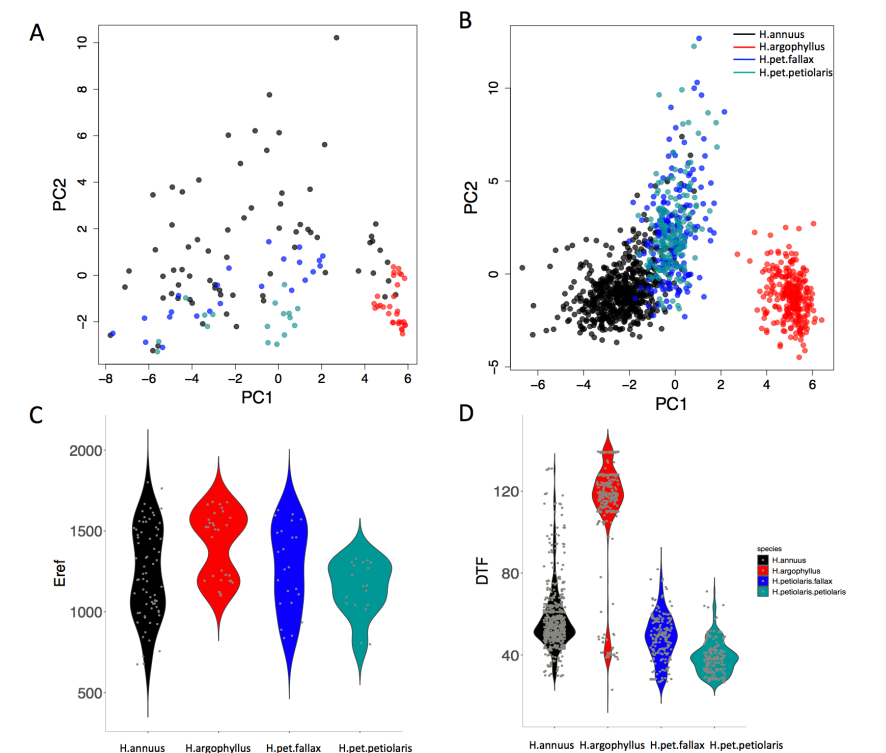
171

172
173
174
175   **Figure 2. The range of environmental and phenotypic overlaps among studied species.**
176   Principle component analysis (PCA) indicating how different species span the range of
177   environmental and phenotypic space, respectively (a, b). Violin plots show two examples of
178   variation in environment (Hargreaves reference evapotranspiration index; Eref) and phenotype
179   (Days to Flower; DTF) within and among the taxa (c,d).

180

181

182   **Genome-wide analysis of repeated local adaptation.** To search for regions of the genome with

183   signatures of repeated adaptation in multiple taxa, we first identified windows of the genome

184   within each species that showed strong signatures of association to either phenotype (GWAS) or

7

185   environment (GEA), referred to as "top candidate" windows. To identify Windows of Repeated

186   Association (WRAs) between pairs of species, we then assessed whether top candidate windows

187   identified in one focal taxon also tended to be enriched for strong signatures of association to the

188   same environment or phenotype in each of the other taxa (using the null-W test, which tends to

189   be more sensitive than just finding the overlap between the top candidate windows; See

190   Methods). As recombination rate can affect the sensitivity of these kinds of window-based

191   genome scans (Booker et al. 2020), the identification of WRAs was conducted after binning

192   windows by recombination rate, although in many cases we did not observe substantial

193   differences in the null distributions among these bins (*e.g.*, Figure S3). This analysis revealed

194   many windows with signatures of repeated association, with the strongest repeated signature

195   found for Number of Frost-Free Days (NFFD; Figure 3A; S4), but also showed that many of the

196   windows with the strongest association in one species did not have strong signatures in other

197   species (Figure 3B).
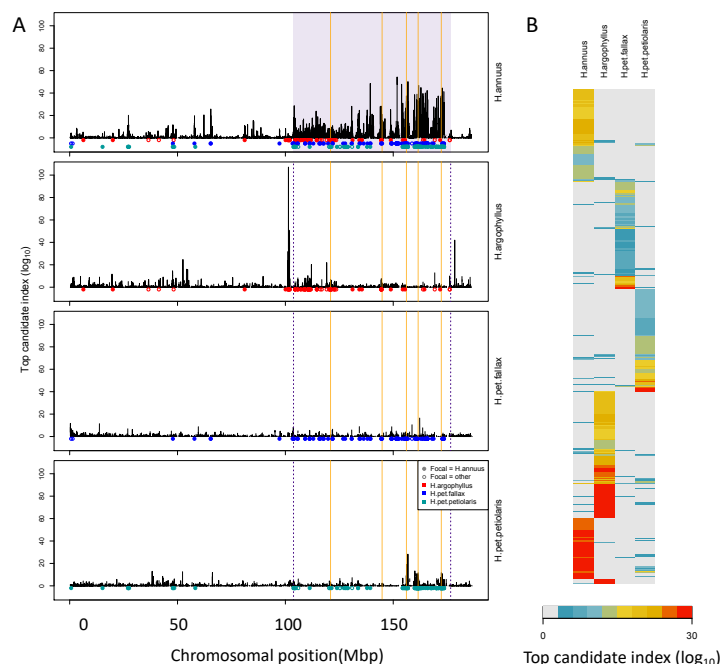
198

199

200   Figure 3. Signatures of association for Number of Frost-Free Days (NFFD) in the four taxa on

201   chromosome 15 (A) and genome-wide (B). Panel A shows Windows of Repeated Association

202   (WRAs; coloured bars) for comparisons between the focal speces, *H. annuus*, and each of the

203   other 3 taxa, with the haploblocks in *H. annuus* shaded in violet and the regions with significant

8

204   PicMin hits as vertical orange lines. Panel B shows the value of the top candidate index for each

205   of the 1000 windows with the strongest signatures of association in at least one species, ordered

206   by clustering to group windows with similar patterns across multiple species.

207

208   Under the null hypothesis that all regions of the genome evolve neutrally due to drift and

209   independently in each species, ~5% of the top candidate windows identified in one species

210   would be expected to fall into the tail of the null distribution of another species (i.e. be classified

211   as WRAs). While we find significantly more WRAs than the 5% expected by chance, ranging

212   from 6.3% to 44.1% (mean = 14.5%; Figure S4), multiple factors can violate the assumptions of

213   this test and increase the proportion of windows classified as WRAs. Most importantly,

214   similarity in signatures of association can be driven by shared ancestral variation or ongoing

215   introgression, and this must always be considered as an alternative explanation. It is clear that

216   most regions of the genome harbour some shared standing variation between all 6 pairwise

217   comparisons of the taxa, whether due to segregating ancestral variation or introgression, based

218   on an index quantifying the proportion of shared to non-shared SNPs in each window (Figure

219   S5). However, we do not find consistent differences in the amount of shared standing variation

220   within windows when comparing WRAs with the rest of the genome (Figure S5). Thus, while

221   introgression may make subtle contributions to WRAs, a lack of increased shared standing

222   variation in the significant windows suggests that it is not a primary driver of these patterns.

223   A second source of inflation in the number of WRAs is due to hitchhiking: if a given

224   locus is a true positive driving adaptation, LD with other windows in tight physical linkage will

225   result in spurious correlations causing them to also be classified as WRAs increasing the

226   genome-wide proportion above 5%, and this effect will be particularly exaggerated in

227   haploblocks. To control for this, we binned neighbouring WRAs together that exhibited high LD

228   (>95th percentile) over short spans of the genome (<1 cM) in either species, yielding regions we

229   refer to as Clusters of Repeated Association (CRAs). While this clustering method should

230   provide a partial control for the effect of hitchhiking, we note that the number of CRAs cannot be

231   taken as a reliable estimate of the number of independent targets of natural selection. Instead, we

232   treat the number and size of these CRAs as proxies for the relative genome-wide similarity in

233   association between each pair of species, and conduct downstream analyses to test hypotheses

234   about the factors driving local adaptation.

9

235   CRAs varied in number and size across the 6 pairwise-species comparisons, with

236   particularly large CRAs identified at the sites of known haploblocks (Todesco et al. 2020). For

237   CRAs identified for phenotypic associations, their extent ranged from 168 clusters spanning

238   48,524,903 bp (covering only 1.6% of the genome) in *H.argophyllus-H.pet.petiolaris* to a

239   maximum of 1,667 clusters spanning 426,409,647 bp (14.2 % of the genome) in *H. pet.*

240   *petiolaris-H. pet. fallax* (Figure S6). CRAs identified for environmental variables tended to be

241   more numerous and cover a larger region of the genome, varying from 1154 clusters comprising

242   15% of the total genome for *H. argophyllus-H. pet. fallax* up to 2,260 distinct clusters covering

243   29% of the genome between *H. petiolaris* subspecies (Figure S7). When we use an approach that

244   corrects for population structure in the genotype-environment association tests (Baypass), we

245   find substantially reduced numbers of CRAs (Figure S8), likely due to reduced power to detect

246   true positive causal loci when population structure covaries with environment (as true positives

247   do not "stand out" relative to the genomic background).

248

249   **Repeated association in the genome reflects patterns at the phenotypic level.** If natural

250   selection is driving repeated patterns of local adaptation in the genomes of two species, we

251   should see greater similarity for associations with environmental variables that are also strongly

252   associated with phenotypic variation in both species. Consistent with this prediction, we found

253   that environmental variables with a high SIPEC index (i.e. high correlation with phenotypes;

254   Figure S2) also tended to have a larger number of CRAs in all comparisons (Figure 4), with

255   higher repeatability at both the phenotype and genome level for temperature-related variables

256   and much lower repeatability for soil-related variables. Unfortunately, given the non-

257   independence of environmental variables it is not possible to conduct a formal significance test

258   of these patterns. In all cases, the number of CRAs exhibited a weak negative relationship with

259   the index of standing variation, with environmental variables that had the greatest number of

260   CRAs having the lowest relative amounts of shared standing variation (Figure S9). This suggests

261   that the observed similarity in patterns of association among species is not being strongly driven

262   by incomplete lineage sorting or introgression, as we would expect a positive relationship

263   between the index of shared standing variation and the number of CRAs. We found similar but

264   weaker patterns in the association between SIPEC and size of CRAs (Figure S10), which may

265   reflect comparatively greater contribution of haploblocks driving patterns with size rather than

10

266   number (i.e. if a particularly large haploblock is a CRA, then that variable will have a

267   particularly large value relative to its actual importance for local adaptation).
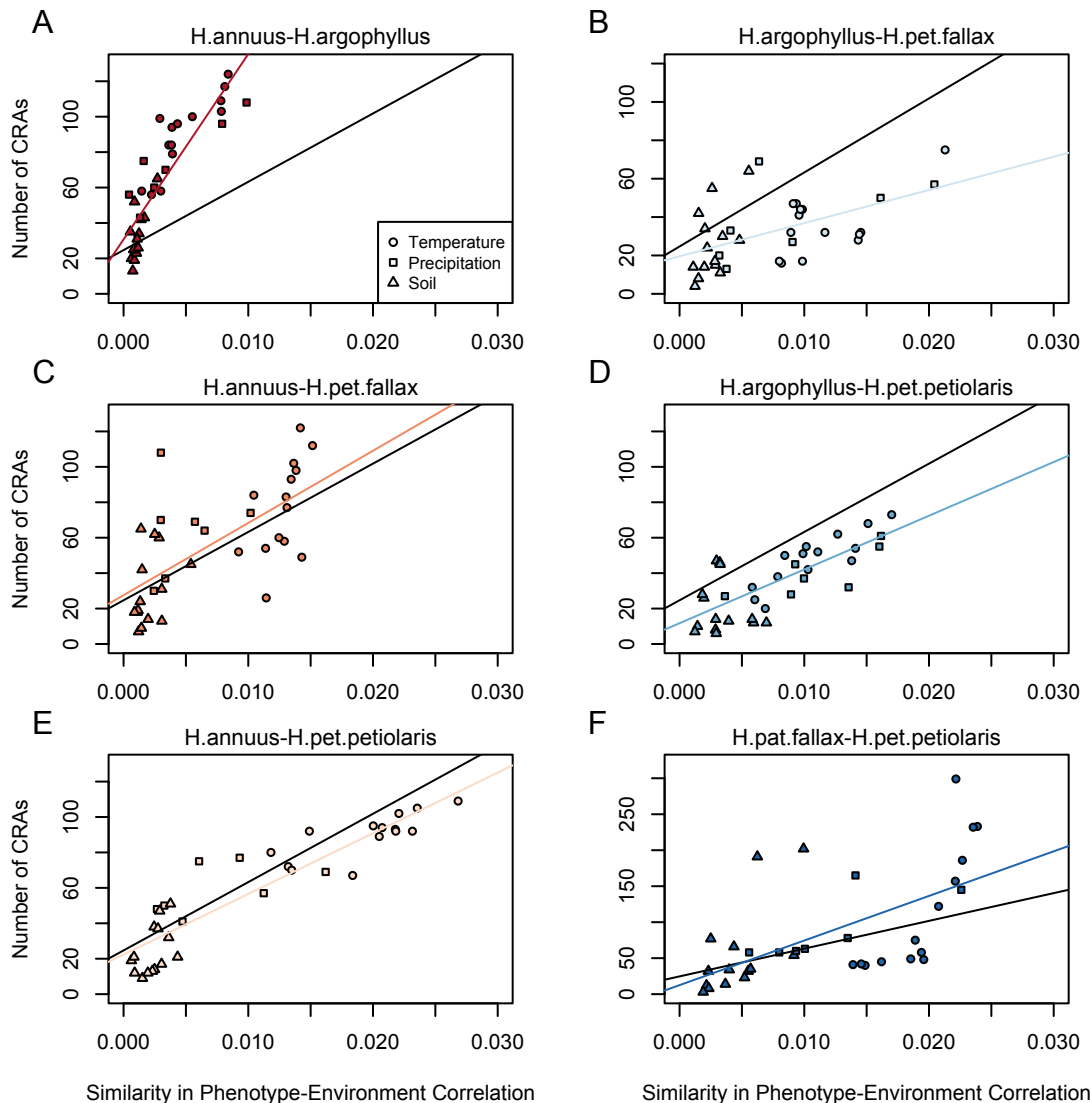
268

269
270
271   Figure 4. Relationship between mean Similarity in Phenotype-Environment Correlation (SIPEC)
272   and number of Clusters of Repeated Association (CRAs). Each panel includes both a linear
273   model fit to the data within the panel (coloured lines), and a linear model fit to all data
274   simultaneously (black lines) for comparison.

275

276

Overlap of signatures of repeated association with low recombination haploblocks.

Inversions can facilitate local adaptation by suppressing recombination between locally adapted alleles within the inverted vs. ancestral haplotypes (Kirkpatrick and Barton 2006). If a given species exhibits a signature of association to environment at a segregating inversion, it is interesting to test whether similar signatures of association are found in other species at the same region of the genome that lack a segregating inversion. This would suggest that particularly strong selection is acting on this region, as signatures of association can still evolve even without the recombination suppressing effect of the inversion. While not all of the low-recombination haploblocks identified by Todesco et al. (2020) have been validated as inversions, for simplicity we treat each haploblock as representative of a segregating inversion. The majority of these haploblocks are present as segregating variation in only one of the three species, but when they occur in *H. petiolaris*, they tend to be found as segregating variation within both subspecies. Thus, if we find significant enrichment of the regions of repeated association (WRAs and CRAs) within haploblocks, this suggests that both the species with a segregating inversion and the species lacking an inversion are using this region of the genome to drive local adaptation. As a first test of this relationship, we assessed two-way contingency tables for whether top candidate windows within a species were also significant windows of repeated association (WRA/non-WRA) and whether they fell within haploblocks (yes/no). This approach controls for the potential enrichment of top candidate windows within haploblocks relative to the rest of the genome and asks if the rate of WRAs within haploblocks is higher. For most phenotypes and environments, we found that the proportion of WRAs in haploblocks was much higher than for non-WRAs (Figure 5). Across all species comparisons and environmental/phenotypic variables, a total of 310 contrasts showed significant enrichment for WRAs in haploblocks, compared to only 23 contrasts showing a significantly higher proportion of non-WRAs in haploblocks. In *H. argophyllus*, while non-WRA top candidates tended to fall within haploblocks less commonly than in the other taxa, WRAs tended to be very strongly enriched within haploblocks (Figure 5B). As a follow-up, we also tested whether CRAs were enriched within haploblocks (without controlling for whether top candidate windows also tended to be enriched), also finding strongly significant enrichment of CRAs within haploblocks for many traits and environments (Figure S6C & D). Broad patterns revealed by these analyses are similar, as both show that regions with haploblocks tend to be enriched for signatures of association to environment in species lacking

12

308   the haploblock. It is noteworthy that few significant signatures of enrichment in haploblocks

309   were found for *H. petiolaris petiolaris* vs. *H. petiolaris fallax* (Figure S6C & D), perhaps

310   because extensive introgression across non-locally adapted regions of the genome obscures true
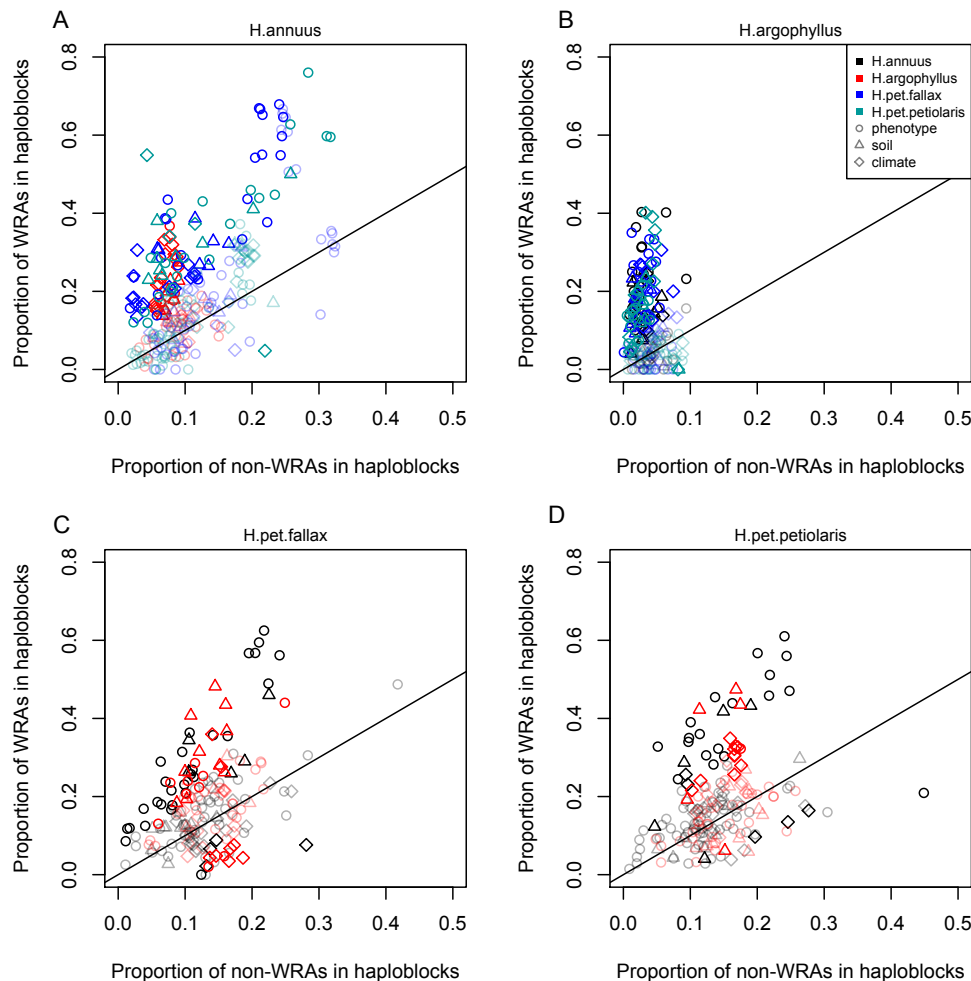
311   signal.

312

313
314
315   Figure 5. Enrichment of signatures of repeated association within genomic regions harbouring a
316   haploblock in one of the two compared lineages. Each panel shows the proportion of top
317   candidate genes that fall within haploblocks for windows with significant signatures of repeated
318   association by the null-W test (WRAs) vs. those with non-significant signatures (non-WRAs).
319   Comparisons of *H. petiolaris petiolaris* vs. *H. petiolaris fallax* are omitted as they share
320   segregating haploblocks. Each point corresponds to the results for a single phenotype or
321   environment, with dark shading used for cases where the deviation from random for the
322   contingency table is significant by a permutation test ($p < 0.05$), and lighter shading indicating a
323   non-significant result.
324

325

13

326 **Multi-species signatures of repeated association.** As a complement to the pair-wise analyses

327 described above, we also conducted an analysis using PicMin, which simultaneously considers

328 any number of lineages to identify genes with particularly strong and repeated signatures of

329 association (Booker et al. 2022). After clustering together windows < 1 Mbp apart, we found a

330 total of 145 regions that were significant for at least one variable or phenotype (at FDR < 0.1

331 applied within each variable). The largest number of significant regions for environment was

332 found with the Number of Frost-Free Days variable (20 with FDR < 0.1; 44 with FDR < 0.2) and

333 for phenotypes with Total Leaf Number (9 with FDR < 0.1; 19 with FDR < 0.2). Considering the

334 720 individual 5000 bp windows with FDR < 0.2 for at least one variable, 387 are within 500 bp

335 of a genic region, representing a 2.3x enrichment relative to the rate for windows that were not

336 significant hits using PicMin (23.3% of other windows fall within 500 bp of a genic region; X^2

337 test $p < 10^{-15}$).

338

339

340

341 **Estimating the number of potentially adaptive loci.** Even for the environment with the highest

342 repeatability (Number of frost-free days; NFFD), most of the strongest signals of association are

343 found in only one lineage (Figure 3B). This implies that there is considerable genotypic

344 redundancy, with many different ways for these species to adaptively respond to variation in the

345 same environment. To estimate the number of windows that could potentially contribute to local

346 adaptation for each variable (L_{eff}), we modified the method of Yeaman et al. (2018) to partially

347 account for the effect of linkage among nearby windows (see methods). This method assumes

348 that the windows with signatures of adaptation in each species are a random draw from a larger

349 number of potentially contributing windows (L_{eff}), which can be inferred based on the ratio of

350 shared vs. non-shared windows with strong association signatures (see Methods). We find that

351 estimates of L_{eff} tend to be large, always well over 1000 windows regardless of the trait or

352 environment (Figure S13A). There are numerous sources of error that affect the estimation of

353 L_{eff}, which will tend to be overestimated due to linkage (Figure S13A) or when many signatures

354 of adaptation are false positives (see supplementary results), and will be underestimated when

355 some repeatability is due to shared standing variation (Yeaman et al. 2018). Even after controls

356   for linkage and assuming a high false positive rate of 80%, estimates of L_{eff} remain in the

357   hundreds even for the variable with the lowest value of L_{eff} (Eref; Figure S13C, D).

358

Discussion

360   Despite its critical importance in shaping the architecture of adaptation, little is known about the

361   extent of genotypic redundancy underlying different traits (Barghi et al. 2020; Láruson et al.

362   2020; Yeaman 2022). Here, we have shown evidence of significant repeatability in the basis of

363   local adaptation (Figure 4, 5), but also an abundance of species-specific, non-repeated signatures

364   (Figure 3; S13). In particular, we find that regions of the genome that harbour inversions in one

365   species also tend to be strongly enriched for signatures of adaptation in other species lacking the

366   inversion (Figure 5). Taken together, this suggests that local adaptation in these species is highly

367   flexible -- different species apparently use quite different sets of loci to adapt to the same

368   environment -- yet still involves some component that has minimal redundancy, with inversions

369   playing a particularly important role. Some of the "usual suspects" show up in the set of

370   significantly repeated loci identified by PicMin: in addition to the homologs of the *FT*

371   (*FLOWERING LOCUS T*) gene reported by (Todesco et al. 2020), we also found hits for several

372   other genes involved in circadian regulation and flowering time, including *PRR3* (Para et al.

373   2007)), *TOE1* (Aukerman and Sakai 2003), and *PHYC* (Takano et al. 2005; Chen et al. 2014),

374   which is known to regulate photoperiodic responses in Arabidopsis accessions (Balasubramanian

375   et al. 2006). Other top hits included genes involved in plant development and auxin transport

376   (*PIN3*; (Keuskamp et al. 2010), *ARF4* (Pekker et al. 2005), and *MN*; (Bhatia et al. 2016)), and

377   plant immunity (*CRK13* (Acharya et al. 2007) and *PRR2* (Cheval et al. 2017))

378   The increased repeatability found in regions of the genome that harbour inversions in only

379   one species is particularly interesting. Inversions are commonly associated with local adaptation

380   (Wellenreuther and Bernatchez 2018), likely because they reduce the rate that recombination

381   breaks up combinations of co-selected alleles (Kirkpatrick and Barton 2006), which perhaps

382   facilitates contributions by alleles that would be individually too weakly selected to overcome

383   swamping by migration (Bürger and Akerman 2011; Yeaman and Whitlock 2011; Schaal et al.

384   2022). Evidence here suggests these regions still tend to contribute to adaptation in the species

385   lacking the recombination-suppressing effect of an inversion, consistent with a strong effect of

386   selection relative to migration on at least one locus in the region. Given that under this model,

387   inversions will be mostly likely to persist if they capture multiple locally adapted alleles, the

388   observation of enrichment of signatures of repeated adaptation within inversions could also

389   explain their long-term persistence. If there is variation across the genome in the density of loci

390   with the potential to be involved in local adaptation, then the evolution and maintenance of

391   locally adaptive inversions would be biased towards co-occuring with the loci most likely to be

392   involved in local adaptation. If the potential for local adaptation is conserved amongst species,

393   then these same regions are more likely to have high repeatability. In this way, repeatability in

394   inversion containing regions may reflect the preferential retention of inversions, as well as the

395   retention of locally adaptive alleles. As an example, chromosome 15 harbours a large (72 Mbp)

396   haploblock in *H. annuus* that is strongly associated with NFFD (number of frost-free days), and

397   also shows some signatures of association in the other taxa, with particularly strong signatures of

398   association on either side of the haploblock in *H. argophyllus* (Figure 3A). Interestingly, loci of

399   repeated association identified by PicMin within this region include two genes whose homologs

400   are known to regulate responses to cold: *COLD-RESPONSIVE PROTEIN KINASE 1,CRPK1*

401   (Liu et al. 2017)) and *LATE ELONGATED HYPOCOTYL, LHY* (Mizoguchi et al. 2002; Dong et

402   al. 2011). While many studies have demonstrated the importance of inversions for adaptation

403   (Wellenreuther and Bernatchez 2018; Hager et al. 2022), to our knowledge only one other study

404   has documented the involvement of the same loci making contributions in the absence of the

405   recombination-suppressing effect of the inversion (Lee et al. 2017). This also highlights how

406   comparative studies of a species lacking an inversion may help identify which genes are driving

407   adaptation in another species with an inversion, as segregating inversions tend to have extensive

408   LD that prevents identification of any potential targets of natural selection within them.

409   While our results suggest a large number of loci can potentially contribute to adaptation,

410   implying high redundancy (Figure 3B; S13), there are several factors that complicate inference.

411   Separating the effects of drift and selection to detect signatures of local adaptation is notoriously

412   difficult, because population structure often covaries with features of the environment that drive

413   adaptation (Lotterhos and Whitlock 2014; Hoban et al. 2016; DeRaad et al. 2021). As found by

414   other analyses (Yeaman et al. 2016; DeRaad et al. 2021), when we use structure correction in our

415   genotype-environment association tests, we find many fewer signatures of repeated association

16

416   (Figure S6 vs. S8), likely due to the reduced power of Baypass to detect true positives when the

417   environment covaries with population structure. Here, we have side-stepped the issues involved

418   in correction for population structure by instead relying on comparisons among species to

419   identify loci with associations more extreme than expected by chance, using the null-W and

420   PicMin tests. This assumes that most loci in the genome are not involved in local adaptation, so

421   that the relatively small proportion that are driving adaptation can therefore be picked out due to

422   their tendency to fall into the tail of the distribution of association statistics. While this approach

423   should be relatively robust for identifying loci with repeated patterns of adaptation, there is no

424   way to formally estimate significance of associations found in only a single species, many of

425   which may be false positives due to covariation of population structure and environment.

426   However, even if we assume that 80% of the observed non-repeated loci are false positives, we

427   still find that estimates of the effective number of loci contributing to adaptation (L_{eff}) are in the

428   hundreds (Figure S13C). As we are unable to detect loci of small effect due to the limited power,

429   our estimates of L_{eff} will also be biased downwards by excluding these potentially important

430   drivers. Finally, it is also difficult to exclude the contribution of introgression or incomplete

431   lineage sorting to the observed signatures repeated association. If a locus tended to be highly

432   introgressed between two species in a restricted region of their range, it is possible it could also

433   covary with environment and therefore result in a signature of repeated association that would be

434   mistakenly interpreted as adaptation. While it is difficult to preclude this from our analysis,

435   regions of the genome with signatures of repeated association do not tend to have higher levels

436   of shared standing variation than background regions (Figure S5), suggesting this is not a broad

437   explanation for our observations. If anything, shared standing variation would be expected to

438   increase repeatability of adaptation (MacPherson and Nuismer 2017), adding further weight to

439   the inference that there is high genotypic redundancy in these species.

440   In general, we find that temperature is the strongest driver of repeated adaptation at both

441   the phenotypic and genomic levels. We quantified local adaptation at the phenotypic level using

442   correlations between traits measured in common gardens and the home environment of the

443   population they were sampled from. Across all phenotypes, these correlations tended to be

444   strongest and most similar among species for temperature variables, particularly in comparisons

445   among *H. annuus* and *H. petiolaris* subspecies (Figure S2). We see similar patterns of

17

446   repeatability reflected in the genome, where temperature variables also tend to have the greatest

447   repeatability (Figure 4). The similarity in these phenotypic and genomic signatures is consistent

448   with an effect of strong selection, as other artefactual or drift-based explanations for repeatability

449   would not be expected to reflect patterns found at the phenotypic level. It should be noted that

450   the reduced importance of soil variables in the SIPEC index might be partly driven by the fact

451   that all traits were measured on above-ground features, due to the difficulty of getting good root

452   phenotypes.

453   Taken together, these results suggest that some fraction of the genome contributes to adaptation

454   with low redundancy and high repeatability (which tend to be enriched within inversions), while

455   the remainder of the adaptive response is driven by loci with high redundancy and species-

456   specific contributions. Models in evolutionary genetics tend to focus on extremes: population

457   genetic approaches explore cases where strong selection deterministically drives a change in

458   allele frequency, whereas quantitative genetic approaches make the infinitesimal assumption that

459   phenotypic change can be realized through small frequency changes at many loci (Barton et al.

460   2017; Barghi et al. 2020; Yeaman 2022). Our results suggest that adaptation is a complex

461   process that does not map cleanly onto the assumptions of either approach, but that at least some

462   component of trait variation experiences sufficiently strong selection to overcome migration and

463   drift and behave in a way approximately consistent with population genetic models. Given the

464   difficulty of rigourously quantifying the contribution of alleles of small effect, it remains an open

465   question what proportion of adaptive response is governmed by loci with dynamical behaviour

466   that follow the infinitesimal assumption. This could perhaps be quantified explicitly by

467   decomposing trait heritabilities as has been done for standing variation in humans (Visscher et al.

468   2017), but this would require a considerable increase in sample size as methods such as GCTA

469   (Yang et al. 2011) do not yield accurate estimates at the sample sizes used here

470

471   **Materials and Methods**

472   **Data collection, common garden, and phenotyping.** Seed samples were collected from 151

473   wild sunflower populations covering most of their native distributions during the summer of

474   2015 (*H. annuus*: 61 populations for GWAS and 71 populations for GEA, *H. petiolaris fallax*: 23

18

475   populations, *H. petiolaris petiolaris:* 18 populations and *H. argophyllus*: 30 populations, Figure

476   1 and Supplementary Table 1). Seeds from ten additional populations of *H. annuus* for the GEA

477   analysis had been previously collected in the summer of 2011. Sample seeds were obtained from

478   randomly chosen mothers, and were first germinated in a greenhouse for two weeks, later moved

479   to an open-sided greenhouse for acclimation. Phenotypic data were collected throughout the

480   growing season, as detailed in Supplementary Table 1. Extensive records of developmental and

481   morphological traits throughout the growth of the plants including leaves, stem, and seeds which

482   were collected and digitally imaged to extract relevant phenotypic data.

483

484   **Similarity in Phenotype-Environment Correlation (SIPEC).** Locally adapted traits tend to

485   exhibit strong correlations between environment and common-garden phenotype, so

486   environments that are important to driving local adaptation should exhibit strong correlations

487   with many traits. As an index to represent the similarity among pairs of species in an

488   environment's average correlation across all measured phenotypes, we calculate SIPEC =

489    $\sum_i (|r_{i,1}| + |r_{i,2}|)|r_{i,1}||r_{i,2}|/n_p$ where $r_{i,1}$ and $r_{i,2}$ are the Pearson correlations between the

490   environment and the ith phenotype in the first and second species, respectively, and n_p is the

491   number of phenotypes. This SIPEC index is maximized when the correlation is large in both

492   species regardless of the direction, so it does not differentiate phenotypically convergent vs.

493   divergent patterns of local adaptation, and provides a means of estimating the relative importance

494   of an environment driving local adaptation across all measured phenotypes. To account for non-

495   independence among traits, for each pair of species we fit a PCA to all measured phenotypes and

496   use the Principal Components that collectively explain 95% of the variance, and calculate SIPEC

497   on the correlations of these variables with environment.

498

499   **Tests of SNP association with environment (GEA) and phenotype (GWAS).** A total of 39

500   environmental variables (21 climatic variables, 3 geographic variables, 15 soil variables

501   Supplementary Table 1) were used for the genotype-environment association analysis (GEA).

502   We refer to the climatic, soil and geographic variables collectively as the "environmental

503   variables", for simplicity. Soil data were collected by taking three to five soil samples collected

504   at each population from across the area in which seeds were collected and submitted to Midwest

505   Laboratories Inc. (Omaha, NE, USA) for analysis. Climate data for each population were

506   collected over a 30-year period (1961-1990) from geographic coordinates of the locations where

507   the samples were collected, using the software package Climate NA (Wang et al. 2012). We used

508   the package BAYPASS version 2.1 (Gautier 2015), which provides a re-implementation of the

509   Bayesian hierarchical model, and explicitly accounts for the covariance structure among the

510   population allele frequencies that originate from the shared history of the populations through the

511   estimation of the population covariance matrix. This renders the identification of SNPs subjected

512   to selection less sensitive to the confounding effect of population demography (Günther and

513   Coop 2013). Population structure was estimated by choosing a random and unlinked set of 10 kb

514   SNPs and running BAYPASS under the core model (*i.e.* no covariates). Then the Bayes factors

515   (BF) were calculated running BAYPASS under the STD covariate model to evaluate association

516   of SNPs with environmental variables (*i.e.* adjusting for population structure). For each SNP, the

517   Bayes factor (denoted BF_{is} as in Gautier 2015) was presented in decibian units (db) via the

518   transformation $10 \log_{10} (BF)$. BF_{is} relies on the importance sampling algorithm proposed by

519   Coop et al., 2010 and uses MCMC samples obtained under the core model. To produce a

520   narrower set of outlier loci, we followed the popular Jeffreys' rule (Jeffreys 1961) that identified

521   outlier loci with $BF \geq 10$. As genome scan methods that correct for population structure can

522   remove some potential signals of local adaption when there is covariation between the

523   demographic history of the species and the environmental variables or phenotypic traits of

524   interest, we also calculated Spearman's rank correlation (ρ, uncorrected GEA) between

525   population allele frequencies for each SNP and each environment variable.

526   GWAS analysis was performed 86, 30 and 69 developmental and morphologic traits in *H.*

527   *annuus, H. argophyllus* and *H. petiolaris,* respectively (Supplementary table 1). 29 variables

528   were measured in all three focal species, and 39 were measured only in *H. annuus* and in *H.*

529   *petiolaris* subspecies (Supplementary table 1). Seed and flower traits could not be collected for

530   *H. argophyllus*, since most plants of this species flowered very late in our common garden, and

531   failed to form fully developed inflorescences and set seeds before temperatures became too low

532   for their survival. Population structure was controlled for in GWAS by including the first three

533   principal components as covariates, as well as an identity-by-state (IBS) kinship matrix

534   calculated by EMMAX (Kang et al. 2010). We ran each trait GWAS using EMMAX

535   (v07Mar2010), as well as the EMMAX module in EasyGWAS (Grimm et al. 2017). For every

536   SNP/peak above the Bonferroni significance threshold, candidate genes were selected within a

537   100 Kb interval centered in the SNP with the lowest p-value, or within the boundaries of the

538   GWAS peak, whichever was larger. All variants used for association were initially filtered for

539   VQSR 90% tranche, and then further filtered to only include bi-allelic SNPs genotyped in $\geq$ 90%

540   of samples and with a minor allele frequency $\geq$ 3%.

541   **Identification of top-candidate windows.** We calculated the bottom 0.01 quantiles for the *p*-

542   values from association tests, Spearman's rank correlation (uncorrected GEA) and GWAS

543   (corrected and uncorrected), yielding two 1% cutoffs. For each environmental and phenotypic

544   variable, we identified all outlier SNPs as those that fell below the respective 1% cutoff. For

545   BayPass, we considered SNPs with Bayes factor $\geq$ 10 as outlier SNPs. For each 5 kb window

546   that we defined across the whole genome, we counted the number of outlier SNPs (*a*) and the

547   total number of SNPs (*n*). To identify top-candidate windows for each variable, we compared the

548   number of outlier SNPs per each 5 kb window to the 0.9999 quantile of the binomial expectation

549   where the expected frequency of outlier SNPs per window is calculated as: $\rho = \sum a_i / n_i$

550   (summation over all 5 kp windows), calculating ρ independently for each environmental and

551   phenotype variable and excluding windows with 0 outliers from the calculation of ρ (as per

552   Yeaman et al. 2016). We also calculated a top candidate index using the same approach to

553   categorize outliers, obtaining a *p*-value for a binomial test for the number of SNPs per window

554   given an expected proportion of outliers (ρ; this *p*-value is not exact due to non-independence of

555   SNPs so we refer to this as an index).

556   Identifying outlier SNPs detected by genome scans from genome-wide distribution without

557   accounting for local recombination rate variation can promote false positive signals in

558   recombination cold spots (i.e., low recombination regions) and be overly conservative in

559   recombination hot spots (i.e., high recombination regions) (Booker et al. 2020). Therefore, to

560   account for local recombination rate variation, all genomic windows were binned by their

561   estimated recombination rates into 5 equally sized bins (bin1: 0-20% quantile, bin2: 20%-40%

562   quantile, bin3: 40%-60% quantile, bin4: 60%-80% quantile, bin5: 80%-100% quantile). For each

563   recombination bin, we estimated expected frequency of SNPs per window (ρ) and calculated cut-

564   off separately. Windows falling above the threshold were identified as top candidate windows.

21

565   **Genome-wide survey of repeatability (null-W test).** To explore repeatable genomic signatures

566   of adaptation for each of the six pairwise contrasts among the 4 taxa (Figure 1), we used the

567   method developed by Yeaman et al. (2016) with some modifications. A common approach is to

568   identify candidates for adaptation independently in each species and then examine the overlap

569   between these lists, however this approach is quite stringent and may miss many interesting

570   signals. The null-W test is more sensitive, as it takes the list of top candidates from one species

571   and tests whether they tend to show more extreme signatures of association than expected by

572   chance. The null-W test is especially favorable when LD increased divergence of SNPs in tight

573   linkage with casual SNPs but did not raise the test values enough for a window to be classified as

574   an outlier according to the binomial test. For each top candidate window that we identified for

575   each focal species in a pair, we refer to the same window in the other species as "top candidate

576   ortholog". The null distribution for each focal species and variable was constructed by randomly

577   sampling 10,000 background SNPs from non-top candidate ortholog windows. For each non-top-

578   candidate window, we then estimated the test statistic (W) for the Wilcoxon-signed rank test vs.

579   the 10,000 background SNPs. This resulted in a null distribution representing the differences

580   between the 10,000 background SNPs and the non-top-candidate ortholog windows. These were

581   then standardized to Z-scores using the method in Whitlock and Schluter (2020):

582     $$Z = \frac{2W - n1n2}{\sqrt{n1n2(n1+n2+1)/3}}$$ (Equation 2)

583

584   where n1 and n2 are the sample sizes being compared. In order to control for heterogeneity in

585   recombination rate and its possible effects on the null distribution, we estimated null distribution

586   for each recombination bin separately (5 in total, see above). We then compared the p-values and

587   bayes factors (BFs) for each focal top-candidate widow to the 10,000 background SNPs,

588   calculating the W statistics and converting into a Z-score. Empirical P-values were then

589   calculated by comparing the Z-score for each top-candidate window to the null distribution.

590   When individual windows had values of W that exceeded the bounds of the null distribution,

591   their empirical p-value was set to the reciprocal of the number of genes in the null distribution.

592   Empirical p-values were converted to q-values for estimation of False Discovery Rate and

593   applied this separately to the empirical p-values for each of the variables. For each species pair,

594   we refer to the windows identified as significant by this test as "Windows of Repeated

595   Association" or WRAs.

596

597   **Linkage disequilibrium and detection of clusters of repeated association.** Linkage

598   disequilibrium among adjacent genomic windows can result in statistical non-independence and

599   similar GEA/GWAS signatures across many windows. To group neighbouring WRAs with

600   similar signatures of repeatability into a single "Cluster of Repeated Association" (CRA), we

601   used the following approach in each pairwise contrast, and for each environmental variable and

602   phenotype: beginning with the first WRA along the chromosome, we compared it to the next

603   closest WRA by calculating the Pearson correlation coefficient (r^2) on the allele frequencies

604   across all pairs of SNPs, and compared this estimate to a null distribution. To construct the null

605   distribution, we generated a distribution of LD measurements between 10,000 randomly chosen

606   windows with the same physical distance as between two WRAs (excluding all WRAs from the

607   null distribution). If the r^2 between the two neighboring WRAs was greater than the 95th

608   percentile of the null distribution, we clustered these two windows together. This process was

609   repeated successively with the next closest neighboring WRA, walking out along the

610   chromosome until one of two stopping criteria was reached: 1) the LD between the last two

611   windows did not exceed the 95 percent of the tail distribution or 2) the distance between the

612   initial window and the current window next to it was larger than 1 cM, based on the linkage map

613   from Todesco et al. (2020). When the first round of clustering stopped due to either of these two

614   criteria, all the clustered windows were removed from the dataset and the process started with the

615   second smallest empirical p-value. By doing this way, each WRA will only appear in a single

616   CRA.

617

618   **Estimating an index of shared standing variation.** As genotype calling was conducted

619   separately for each species (due to computational concerns), we estimated the amount of shared

620   standing variation based on counts of shared vs. non-shared SNPs. If two species are evolving

621   independently, the number of shared SNPs should follow a hypergeometric distribution, so we

622   used an approach similar to the C-scores (Yeaman et al. 2018) to calculate the difference

623   between the observed number of shared SNPs and the expectation, scaled by the standard

23

624   deviation of the hypergeometric. Because of noise and a relatively small number of SNPs per

625   window, we applied this approach on a sliding window basis, including the 5 flanking windows

626   upstream and downstream of each focal window the calculation of its index of shared standing

627   variation.

628   **Correspondence between regions of repeated association and chromosomal**

629   **rearrangements.** To assess the extent of overlap between regions of the genome with repeated

630   signatures of association and previously identified low-recombination haploblocks, we used two

631   approaches. Firstly, for each pairwise species contrast and variable, we constructed a

632   contingency table for the number of top candidates that were significant WRAs vs. not-

633   significant WRAs (by the null-W test), and that did vs. did not fall within a haploblock. We

634   calculated the Pearson's χ^2 statistic on this table, and then permuted the location of haploblocks

635   throughout the genome to construct a null distribution of χ^2 statistics, and calculated the p-value

636   as the proportion of the null that exceeded the observed χ^2 statistic (to account for non-

637   independence of nearby WRAs). Secondly, we compared observations of the length and number

638   of overlapping regions to expectations based on a randomization approach. For each pair of

639   species, we kept the position of each CRA constant and randomized the position of haploblocks

640   10,000 times to build a null distribution. By keeping the position of the CRAs constant, we

641   maintained the architecture of adaptation independent from chromosomal rearrangements. We

642   assessed significance by testing whether the observed overlaps between CRAs and haploblocks

643   were more extreme than the 95th percentile of the tail of null distribution. Details about

644   identifying chromosomal rearrangements can be found in Todesco et al. (2020).

645   **Identifying repeated signatures of association across all taxa**. As a complement the the

646   pairwise analysis, we used PicMin (Booker et al. 2022) to identify windows of the genome with

647   strong signatures of association in multiple (sub-) species. For each environmental variable,

648   association signatures for each window are ranked genome-wide and PicMin identifies windows

649   with extreme ranks in multiple species. We ran the analysis once with each of the two 3-way

650   comparisons involving one *petiolaris* subspecies (i.e. *H. annuus, H. argophyllus,* and either *H.*

651   *pet. petiolaris* or *H. pet. fallax*) to control for repeatability arising from similar patterns in the

652   two *petiolaris* subspecies (due to high introgression/shared standing variation).

653 **Evaluating genotypic redundancy using C-scores.** Genome-wide quantification of the
654 repeatability of association statistics provides insights into the amount of genotypic redundancy
655 underlying a trait or environmental adaptation, and can be assessed using the C-score approach
656 (Yeaman et al. 2018). Briefly, for a given trait or environment, the set of association test scores
657 within each species is classified into "associated" or "non-associated" using the binomial top
658 candidate approach. For a given pair of species ($i = 1, 2$), the observed number of associated
659 windows in each species (a_1, a_2) can be compared to the number of windows that are associated
660 in both species (a_b) and the total number of windows being analysed (a_x). Under a null
661 hypothesis where all windows in the genome have equal potential to be involved in adaptation
662 (i.e. associated with the trait or environment), the expected number of windows associated in
663 both species will be described by a hypergeometric distribution, with the expectation $\overline{a_b} =$
664 $a_1 a_2 / a_x$. The difference between the observed and expected amount of overlap in association
665 scores can be quantified as a C-score by scaling the difference by the standard deviation of the
666 hypergeometric (i.e. a C-score of 2 means that the observed amount of overlap is two standard
667 deviations above the expectation under randomness).
668   We assess the C-scores for each phenotype and environment trait by classifying the top
669 0.5% of all 5 kb windows within each species as "associated" (a_i; based on the binomial top
670 candidate index), and begin by calculating the C-score obtained when a_x is set to the union of a_i
671 across all four focal species/sub-species (i.e. only those windows associated in at least one
672 species are included in a_x, a number much lower than the total number of windows in the
673 genome). This yields a negative C-score, as a random draw from such a small number of
674 windows tends to yield many more overlapping associations by chance than the observation.
675 When the C-score = 0, it means that the observed overlap between the pair of taxa being
676 considered is consistent with a random draw of their respective "associated" windows from an
677 overall pool of a_x windows. Thus, by adding rows to the matrix with "non-associated" scores for
678 all 4 species/sub-species until finding the matrix that yields C-score = 0, we can estimate the
679 effective number of loci that contributed to variation for the trait or environment being
680 considered (L_{eff}), under the assumption that all such $a_x = L_{eff}$ windows had an equal chance of
681 contributing to the associations.
682   To run the C-score analysis on LD-clustered windows, we ran the following algorithm for
683 each trait/environmental variable: for each species, we identified all CRAs that also had a top

25

684   candidate index in top 0.5%. In most cases, a large cluster with associated windows in one

685   species corresponds to either no clusters or a small cluster in another species. To harmonize

686   cluster boundaries across species, we bin any overlapping clusters together to their maximum

687   extent, and take the average top candidate index for each cluster in each species as either: (a) the

688   mean across all windows that were "associated" in that species or (b) the average across all

689   windows associated in any species, if no windows were associated in that species. This yields a

690   matrix that can be submitted to the hypergeometric C-score analysis.

691

Data availability

693   All scripts used for analysis and figures will be deposited in a Dryad archive along data files and

694   results. Raw sequence data are deposited in the Sequence Read Archive (SRA) under BioProject

695   accessions PRJNA532579, PRJNA398560, and PRJNA564337, as described in Todesco et al.

696   (2020).

697

704

705

706

707

References:

Acharya BR, Raina S, Maqbool SB, Jagadeeswaran G, Mosher SL, Appel HM, Schultz JC, Klessig DF, Raina R. 2007. Overexpression of CRK13, an Arabidopsis cysteine-rich receptor-like kinase, results in enhanced resistance to Pseudomonas syringae: Overexpression of CRK13 induces pathogen defense. *The Plant Journal* 50:488–499.

Auge GA, Penfield S, Donohue K. 2019. Pleiotropy in developmental regulation by flowering-pathway genes: is it an evolutionary constraint? *New Phytol* 224:55–70.

Aukerman MJ, Sakai H. 2003. Regulation of Flowering Time and Floral Organ Identity by a MicroRNA and Its *APETALA2* -Like Target Genes. *Plant Cell* 15:2730–2741.

Balasubramanian S, Sureshkumar S, Agrawal M, Michael TP, Wessinger C, Maloof JN, Clark R, Warthmann N, Chory J, Weigel D. 2006. The PHYTOCHROME C photoreceptor gene mediates natural variation in flowering and growth responses of Arabidopsis thaliana. *Nat Genet* 38:711–715.

Barghi N, Hermisson J, Schlötterer C. 2020. Polygenic adaptation: a unifying framework to understand positive selection. *Nat Rev Genet* 21:769–781.

Barton NH, Etheridge AM, Véber A. 2017. The infinitesimal model: Definition, derivation, and implications. *Theoretical Population Biology* 118:50–73.

Bhatia N, Bozorg B, Larsson A, Ohno C, Jönsson H, Heisler MG. 2016. Auxin Acts through MONOPTEROS to Regulate Plant Cell Polarity and Pattern Phyllotaxis. *Current Biology* 26:3202–3208.

Blackman BK, Scascitelli M, Kane NC, Luton HH, Rasmussen DA, Bye RA, Lentz DL, Rieseberg LH. 2011. Sunflower domestication alleles support single domestication center in eastern North America. *Proc. Natl. Acad. Sci. U.S.A.* 108:14360–14365.

Bohutínská M, Vlček J, Yair S, Laenen B, Konečná V, Fracassetti M, Slotte T, Kolář F. 2021. Genomic basis of parallel adaptation varies with divergence in *Arabidopsis* and its relatives. *Proc. Natl. Acad. Sci. U.S.A.* 118:e2022713118.

Booker TR, Yeaman S, Whitlock MC. 2020. Variation in recombination rate affects detection of outliers in genome scans under neutrality. *Mol Ecol* 29:4274–4279.

Booker TR, Yeaman S, Whitlock MC. 2022. Using genome scans to identify genes used repeatedly for adaptation. Evolutionary Biology Available from: http://biorxiv.org/lookup/doi/10.1101/2022.03.24.485690

Bürger R, Akerman A. 2011. The effects of linkage and gene flow on local adaptation: A two-locus continent–island model. *Theoretical Population Biology* 80:272–288.

741 Chen A, Li C, Hu W, Lau MY, Lin H, Rockwell NC, Martin SS, Jernstedt JA, Lagarias JC,
742   Dubcovsky J. 2014. PHYTOCHROME C plays a major role in the acceleration of wheat
743   flowering under long-day photoperiod. *Proc. Natl. Acad. Sci. U.S.A.* 111:10037–10044.

744 Cheval C, Perez M, Leba LJ, Ranty B, Perochon A, Reichelt M, Mithöfer A, Robe E, Mazars C,
745   Galaud JP, et al. 2017. PRR2, a pseudo-response regulator, promotes salicylic acid and
746   camalexin accumulation during plant immunity. *Sci Rep* 7:6979.

747 DeRaad DA, Cobos ME, Alkishe A, Ashraf U, Ahadji-Dabla KM, Nuñez-Penichet C, Peterson
748   AT. 2021. Genome-environment association methods comparison supports omnigenic
749   adaptation to ecological niche in malaria vector mosquitoes. *Molecular Ecology*
750   30:6468–6485.

751 Dong MA, Farré EM, Thomashow MF. 2011. CIRCADIAN CLOCK-ASSOCIATED 1 and
752   LATE ELONGATED HYPOCOTYL regulate expression of the C-REPEAT BINDING
753   FACTOR (CBF) pathway in *Arabidopsis*. *Proc. Natl. Acad. Sci. U.S.A.* 108:7241–7246.

754 Gautier M. 2015. Genome-Wide Scan for Adaptive Divergence and Association with
755   Population-Specific Covariates. *Genetics* 201:1555–1579.

756 Grimm DG, Roqueiro D, Salomé PA, Kleeberger S, Greshake B, Zhu W, Liu C, Lippert C,
757   Stegle O, Schölkopf B, et al. 2017. easyGWAS: A Cloud-Based Platform for Comparing
758   the Results of Genome-Wide Association Studies. *Plant Cell* 29:5–19.

759 Günther T, Coop G. 2013. Robust Identification of Local Adaptation from Allele Frequencies.
760   *Genetics* 195:205–220.

761 Hager ER, Harringmeyer OS, Wooldridge TB, Theingi S, Gable JT, McFadden S, Neugeboren
762   B, Turner KM, Jensen JD, Hoekstra HE. 2022. A chromosomal inversion contributes to
763   divergence in multiple traits between deer mouse ecotypes. *Science* 377:399–405.

764 Heiser C, Smith D, Clevenger S, Martin W. 1969. The North American sunflowers (Helianthus).
765   *Memoirs of the Torrey Botanical Club* 22:1–218.

766 Heiser, CB. 1951. Hybridization in the Annual Sunflowers: Helianthus annuus x H. argophyllus.
767   *The American Naturalist* 85:65–72.

768 Hoban S, Kelley JL, Lotterhos KE, Antolin MF, Bradburd G, Lowry DB, Poss ML, Reed LK,
769   Storfer A, Whitlock MC. 2016. Finding the Genomic Basis of Local Adaptation: Pitfalls,
770   Practical Solutions, and Future Directions. *The American Naturalist* 188:379–397.

771 Izawa T. 2007. Adaptation of flowering-time by natural and artificial selection in Arabidopsis
772   and rice. *Journal of Experimental Botany* 58:3091–3097.

773 Jeffreys H. 1961. Theory of probability. 3rd ed. New York, NY: Oxford University Press

Kang HM, Sul JH, Service SK, Zaitlen NA, Kong S, Freimer NB, Sabatti C, Eskin E. 2010. Variance component model to account for sample structure in genome-wide association studies. *Nat Genet* 42:348–354.

Keuskamp DH, Pollmann S, Voesenek LACJ, Peeters AJM, Pierik R. 2010. Auxin transport through PIN-FORMED 3 (PIN3) controls shade avoidance and fitness during competition. *Proc. Natl. Acad. Sci. U.S.A.* 107:22740–22744.

Kirkpatrick M, Barton N. 2006. Chromosome Inversions, Local Adaptation and Speciation. *Genetics* 173:419–434.

Láruson ÁJ, Yeaman S, Lotterhos KE. 2020. The Importance of Genetic Redundancy in Evolution. *Trends in Ecology & Evolution* 35:809–822.

Lee C-R, Wang B, Mojica JP, Mandáková T, Prasad KVSK, Goicoechea JL, Perera N, Hellsten U, Hundley HN, Johnson J, et al. 2017. Young inversion with multiple linked QTLs under selection in a hybrid zone. *Nat Ecol Evol* 1:0119.

Liu Z, Jia Y, Ding Y, Shi Y, Li Z, Guo Y, Gong Z, Yang S. 2017. Plasma Membrane CRPK1-Mediated Phosphorylation of 14-3-3 Proteins Induces Their Nuclear Import to Fine-Tune CBF Signaling during Cold Response. *Molecular Cell* 66:117-128.e5.

Lotterhos KE, Whitlock MC. 2014. Evaluation of demographic history and neutral parameterization on the performance of F_{ST} outlier tests. *Mol Ecol* 23:2178–2192.

MacPherson A, Nuismer SL. 2017. The probability of parallel genetic evolution from standing genetic variation. *J. Evol. Biol.* 30:326–337.

Manceau M, Domingues VS, Linnen CR, Rosenblum EB, Hoekstra HE. 2010. Convergence in pigmentation at multiple levels: mutations, genes and function. *Phil. Trans. R. Soc. B* 365:2439–2450.

Mizoguchi T, Wheatley K, Hanzawa Y, Wright L, Mizoguchi M, Song HR, Carré IA, Coupland G. 2002. LHY and CCA1 are partially redundant genes required to maintain circadian rhythms in Arabidopsis. *Dev Cell* 2:629–641.

Moyers BT, Rieseberg LH. 2016. Remarkable life history polymorphism may be evolving under divergent selection in the silverleaf sunflower. *Mol Ecol* 25:3817–3830.

Ostevik KL, Andrew RL, Otto SP, Rieseberg LH. 2016. Multiple reproductive barriers separate recently diverged sunflower ecotypes: reproductive barriers between sunflower ecotypes. *Evolution* 70:2322–2335.

Para A, Farré EM, Imaizumi T, Pruneda-Paz JL, Harmon FG, Kay SA. 2007. PRR3 Is a vascular regulator of TOC1 stability in the Arabidopsis circadian clock. *Plant Cell* 19:3462–3473.

Pekker I, Alvarez JP, Eshed Y. 2005. Auxin response factors mediate Arabidopsis organ asymmetry via modulation of KANADI activity. *Plant Cell* 17:2899–2910.

809 Rosenblum EB, Parent CE, Brandt EE. 2014. The Molecular Basis of Phenotypic Convergence.
810   *Annu. Rev. Ecol. Evol. Syst.* 45:203–226.

811 Sambatti JBM, Strasburg JL, Ortiz-Barrientos D, Baack EJ, Rieseberg LH. 2012. Reconciling
812   extremely strong barriers with high levels of gene exchange in annual sunflowers: gene
813   flow across a strong reproductive barrier. *Evolution* 66:1459–1473.

814 Schaal SM, Haller BC, Lotterhos KE. 2022. Inversion invasions: when the genetic basis of local
815   adaptation is concentrated within inversions in the face of gene flow. *Phil. Trans. R. Soc.*
816   *B* 377:20210200.

817 Strasburg JL, Rieseberg LH. 2008. Molecular demographic history of the annual sunflowers
818   *helianthus annuus* and *h. Petiolaris* -large effective population sizes and rates of long-
819   term gene flow. *Evolution* 62:1936–1950.

820 Takano M, Inagaki N, Xie X, Yuzurihara N, Hihara F, Ishizuka T, Yano M, Nishimura M,
821   Miyao A, Hirochika H, et al. 2005. Distinct and Cooperative Functions of Phytochromes
822   A, B, and C in the Control of Deetiolation and Flowering in Rice. *The Plant Cell*
823   17:3311–3325.

824 Tittes S, Lorant A, McGinty S, Doebley JF, Holland JB, Sánchez-González J de J, Seetharam A,
825   Tenaillon M, Ross-Ibarra J. 2021. Not so local: the population genetics of convergent
826   adaptation in maize and teosinte. Evolutionary Biology Available from:
827   http://biorxiv.org/lookup/doi/10.1101/2021.09.09.459637

828 Todesco M, Owens GL, Bercovich N, Légaré J-S, Soudi S, Burge DO, Huang K, Ostevik KL,
829   Drummond EBM, Imerovski I, et al. 2020. Massive haplotypes underlie ecotypic
830   differentiation in sunflowers. *Nature* 584:602–607.

831 Visscher PM, Wray NR, Zhang Q, Sklar P, McCarthy MI, Brown MA, Yang J. 2017. 10 Years
832   of GWAS Discovery: Biology, Function, and Translation. *The American Journal of*
833   *Human Genetics* 101:5–22.

834 Wang L, Josephs EB, Lee KM, Roberts LM, Rellán-Álvarez R, Ross-Ibarra J, Hufford MB.
835   2021. Molecular Parallelism Underlies Convergent Highland Adaptation of Maize
836   Landraces.Purugganan M, editor. *Molecular Biology and Evolution* 38:3567–3580.

837 Wang T, Hamann A, Spittlehouse DL, Murdock TQ. 2012. ClimateWNA—High-Resolution
838   Spatial Climate Data for Western North America. *Journal Of Applied Meteorology And*
839   *Climatology* 51:14.

840 Wellenreuther M, Bernatchez L. 2018. Eco-Evolutionary Genomics of Chromosomal Inversions.
841   *Trends in Ecology & Evolution* 33:427–440.

842 Whitlock M, Schluter D. 2020. The analysis of biological data. 3rd ed. Macmillan

843 Yang J, Lee SH, Goddard ME, Visscher PM. 2011. GCTA: A Tool for Genome-wide Complex
844   Trait Analysis. *The American Journal of Human Genetics* 88:76–82.

845   Yeaman S. 2022. Evolution of polygenic traits under global *vs* local adaptation. *Genetics*
846   220:iyab134.

847   Yeaman S, Gerstein AC, Hodgins KA, Whitlock MC. 2018. Quantifying how constraints limit
848   the diversity of viable routes to adaptation.Ralph PL, editor. *PLoS Genet* 14:e1007717.

849   Yeaman S, Hodgins KA, Lotterhos KE, Suren H, Nadeau S, Degner JC, Nurkowski KA, Smets
850   P, Wang T, Gray LK, et al. 2016. Convergent local adaptation to climate in distantly
851   related conifers. *Science* 353:1431–1433.

852   Yeaman S, Whitlock MC. 2011. The genetic architecture of adaptation under migration-selection
853   balance: the genetic architecture of local adaptation. *Evolution* 65:1897–1911.

854

855